IEEE Access
Multidisciplinary ⋮ Rapid Review ⋮ Open Access Journal

Received 10 June 2024, accepted 6 July 2024, date of publication 10 July 2024, date of current version 29 July 2024.

Digital Object Identifier 10.1109/ACCESS.2024.3425907

RESEARCH ARTICLE

Prediction of Dynamic Plantar Pressure From Insole Intervention for Diabetic Patients Based on Patch-Based Multilayer Perceptron With Localization Embedding

LI-YING ZHANG[1,2], ZE-QI MA[1,2], KIT-LUN YICK[1,2], PUI-LING LI[1], JOANNE YIP[1], SUN-PUI NG[3], AND QI-LONG LIU[1]

[1]School of Fashion and Textiles, The Hong Kong Polytechnic University, Hong Kong, China
[2]Laboratory for Artificial Intelligence in Design, Hong Kong Science Park, Hong Kong, China
[3]School of Professional Education and Executive Development, The Hong Kong Polytechnic University, Hong Kong, China

Corresponding author: Kit-Lun Yick (tcyick@polyu.edu.hk)

This work was supported in part by the Laboratory for Artificial Intelligence in Design under Project RP1-2; and in part by The Hong Kong Polytechnic University, Hong Kong, under Project WZ21.

This work involved human subjects or animals in its research. Approval of all ethical and experimental procedures and protocols was granted by the Human Subjects Ethics Sub-Committee of The Hong Kong Polytechnic University under Reference No. HSEARS20200128001.

ABSTRACT Assessing plantar pressure is crucial for fabricating diabetic insoles and preventing diabetic foot ulcers (DFUs), which are caused by increased plantar pressure. However, the commonly used methods for assessing plantar pressure distribution involve professional sensor-based equipment and expertise, which are costly and time-consuming. Given the qualitative association between ink footprint images and plantar pressure, this study proposes using the footprint images to predict the quantitative values of dynamic plantar pressure in barefoot and 4 different insole conditions (including Nora Lunalastik EVA, Nora Lunalight A fresh, Pe-Lite, and PORON® Medical 4708) based on a multilayer perceptron (MLP) neural network model. To provide more precise insole material recommendations for specific foot regions for better plantar pressure distribution, the plantar of the foot is divided into 5 regions: the toes, metatarsal heads, medial midfoot, lateral midfoot, and heel. Patch-based MLP with localization embedding is introduced to learn the correspondence between ink density and plantar pressure information. Ground-truth data collected from 52 diabetes patients is constructed as a dataset named *diabetes-footprint-to-pressure* and used to train and validate the model. The mean absolute error (MAE) of the models for the barefoot and 4 insole conditions is 5.51% (33.06 kPa), 3.99% (23.94 kPa), 4.85% (29.10 kPa), 4.25% (25.50 kPa), and 3.57% (21.42 kPa) of the sensing range, respectively. Compared to traditional methods for plantar pressure assessment, this approach streamlines the process of acquiring the overall and regional dynamic plantar pressure with barefoot and 4 different insole materials. Clinicians can quickly provide recommendations on the type of insole material for individual patients.

INDEX TERMS Diabetes, footprint, insole, multilayer perceptron, plantar pressure.

The associate editor coordinating the review of this manuscript and approving it for publication was Zeev Zalevsky.

I. INTRODUCTION

Abnormal plantar pressure of the foot is one of the underlying risk factors with the development of diabetic foot ulcers (DFUs) [1]. A timely diagnosis and prevention can effectively delay the progression of this condition from reaching to the more severe stages and reducing the risk of complications. Offloading plantar pressure is considered to be an important intervention for preventing DFUs [2], [3]. Appropriate interventions like customised insoles are key prevention strategies to offload abnormal plantar pressure [4], [5], [6]. Nevertheless, the type of insole materials used is particularly critical in the prescription process to achieve optimal offloading [7].

Plantar pressure maps of insoles designed with different types of materials have been used to evaluate the offloading performance [8]. The data obtained from patients and the decision made by physicians are important as resources towards fabricating optimal insole material. Except for evaluating the offloading performance of insoles, plantar pressure distribution is also used to assess the biomechanical function of the foot, e.g. anatomical foot deformities, determine ulcer risk [9], body motion function [10], and compare different footwear/insole effects. Previous works have shown that the reduced plantar pressure in the medial foot during walking would show poor gait balance, thus increasing the fall risk among the elderly [11]. An increase in plantar pressure was found to be mostly in the forefoot region during walking with the progression of diabetic neuropathy [12]. However, the diabetic foot might not be able to sense abnormal plantar pressure due to loss of sensation. Prolonged loading will lead to DFUs if the excessive plantar pressure is not detected and prevented in advance. Therefore, early management and efficient detection of plantar pressure is critical for diabetic feet.

As a low-cost and non-invasive method, ink footprints are widely used to assess the foot type and foot problems in clinical assessment [13], which is particularly suitable for early management and efficient detection of DFUs. There are various methods to obtain the footprints with different instruments, like ink imprint, optical podoscopes, radiography, and platinum scanners [14]. Ink imprint has been widely used due to it is simple and quick to use, cost-effective, and readily available amongst various methods. It not only provides foot shape-related information [15], like the Arch index [16], Staheli index [17], foot contact area, etc. However, though with various advantages, as for the plantar pressure assessment, the ink footprints can only provide qualitative information, i.e. a higher ink density corresponds to a greater plantar pressure. However, the quantitative correlation between the ink density and the plantar pressure is not clear. In clinical practice, clinical experts subjectively identify the plantar pressure pattern based on the ink density distribution and then prescribe the insole structure and materials accordingly [18]. This method is limited and subjective because the ink footprints only qualitatively show the plantar pressure distribution thus the diagnosis result greatly depends on the experience of the clinician.

Developing automatic algorithm to recover the pressure information is particularly difficult, due to the presumably non-linear nature of the pressure-ink density response curve as the pressure increases, the increase of ink density may soon saturate and then reach plateau. If taken the diversity of camera and lightening condition when taking the footprint images into account, the problem becomes even more complicated. To the best of our knowledge, there has not yet been a study to quantitatively predict the plantar pressure from the ink footprints.

Since the advent of machine learning (ML), significant improvement on the tasks that requires high-level pattern recognition, cognitive reasoning, and decision making has been achieved, e.g. image classification [19], [20], [21], [22], object detection [23], [24], [25], instance segmentation [26], [27], and dense human pose estimation [28], [29], [30]. ML's ability to learn hidden patterns from data [31], [32], [33] has drawn to a wide range of applications in disease detection [27], [34], [35], [36] and leads to improvement of efficiency [37], [38], [39], [40].

This study aims at developing a machine learning model to recover the plantar pressure information from the ink footprints and predict the quantitatively pressure distribution with barefoot and 4 different insole conditions for diabetes patients. We first collect footprint images and dynamic plantar pressure distribution data from a group of subjects, constituting a dataset named *diabetes-footprint-to-pressure* that contains 520 pairs of ground-truth footprint-pressure correspondence. We then implement a data augmentation scheme to drastically increase the sample numbers while at the same time avoid hallucinating unrealistic artifacts. These data samples are then used to train a patch-based multilayer perceptron (MLP) model augmented with localization embedding. Though the number of layers and parameters is comparatively small, it is capable to outperform comparison baselines constructed with advanced CNN based architectures [41], [42]. The model is expected to provide a quantitative measure of the plantar pressure, which can be used to assist the clinical experts in the diagnosis of diabetic foot ulcer risk and prescription of the insole structure and materials, thus preventing foot ulcers caused by excessive high plantar pressure and allowing diabetic patients to maintain independence and better quality of life.

II. RELATED WORKS

Plantar pressure measurement systems such as those that are platform-based (F-Scan system) and insole-based (Novel Pedar®) have been traditionally used to evaluate the offloading performance of orthotic insoles [43]. These systems contribute to prescribing orthoses for diabetics to prevent foot ulcers caused by maldistribution of plantar pressure. However, the evaluation process is time consuming [44],

intrusive, and costly, while subjects are burdened with conducting a set of movements repeatedly during walking experiments. Experienced and skilled technicians need to calibrate and manipulate the system which poses a challenge for some clinical practitioners who wish to evaluate the insole performance during the design stage. Additionally, due to the lack of suitable gait measurement equipment in hospitals, inevitably re-measurements and repeated adjustments may take place for insole fitting. Previous analyses of the biomechanical interactions between the foot and the insole are largely based on a finite element analysis (FEA) [45], [46], [47], [48]. The simulation process of foot-insole interaction indeed offers cost-effective results, while the accuracy of the results depends on the geometric model, material properties and meshing density. However, the computational cost of the simulations increases with total number of elements used in the model and the complexity of the analysis, which can limit the utility of finite element modelling in real-time clinical applications [49].

To address the efficiency problem of FEA, Xidias et al. [50] proposed a novel approach to predict the peak plantar pressure of 3 phases of a gait cycle in different insole conditions based on artificial neural networks (ANNs), with a simulated databases created with FEA. The approach provides an accurate (> 96%) and alternative means in comparison to the FEA which incurs a computational cost. However, the accuracy of prediction results from the proposed ANNs model depends on the reliability of the FEA database, while the FEA results depend on multiple factors and reliable results acquisition are quite time-consuming as mentioned in [49]. Another problem of FEA is that it remains unknown whether the results are consistent with the real-world plantar pressure distribution, since FEA is a drastically simplified model of biological tissues and its underlying physical assumptions may not hold for all human subjects in real-world. To address this gap, this research gathers real-world plantar pressure data from human subjects and implements a data augmentation scheme that place particular emphasis on avoiding introducing unrealistic artifacts.

Plantar pressure can also be predicted by using different methods and parameters as is the case in previous studies. Mun and Choi [43] proposed a long short-term memory (LSTM) deep learning model to predict the overall plantar pressure distribution of the stance phase by using a small number of main pressure sensors. Predictors in the regression model proposed by Hazari et al. [51] can explain for 90.8% of the peak plantar pressure. Amongst them, the grades of neuropathy, knee and ankle velocities as well as acceleration have significant contributions to the model. Su et al. [18] also developed an automatic footprint segmentation method for the contact area and arch index calculation and predict the barefoot standing plantar pressure with the mathematical model. However, these prediction methods either need many clinical input predictors [51], [52], [53], [54], like HbA1c, Vibration pressure threshold (VPT), the thickness of plantar fascia or plantar fat pad which also need to measure using professional devices, or only predict the plantar pressure distribution of standing in bare feet condition [18].

Although proposed early in 1940s by McCulloch and Pitts [55], MLP is still widely used in the field of diabetes-related studies. Devarapalli et al. [56] proposed a prototype MLP [57] to use brain derived neurotrophic factor (BDNF) values and other biological variables to predict diabetes. Mohapatra et al. [58] proposed to use 8 attributes of pregnant women for diabetes detection based on MLP. Bani-Salameh et al. [59] compared the correct classification rate (CCR) of an MLP with two other classifiers including support vector machines (SVMs) and K-nearest neighbors (KNNs) and the results show that MLP provides comparatively higher CCR. A similar prediction effectiveness is also showed by Butt et al. [60]. In this research, the MLP model is used to predict the plantar pressure from the ink footprints, with patch-based data augmentation scheme and localization embedding to improve the prediction accuracy. Evaluations showed that though the number of layers and parameters of the proposed network is comparatively small, it is capable to outperform comparison baselines constructed with advanced CNN based architectures [41], [42], indicating advantages in diabetes-related studies and clinical practice.

III. METHOD

A. THE CONSTRUCTION OF DIABETES-FOOTPRINT-TO-PRESSURE DATASET

1) PARTICIPANTS

A total of 52 subjects (26 females, 26 males) who are between 50 and 75 years old (mean = 64, std = 5) with type 1 or type 2 Diabetes Mellitus (DM) were invited to participate in this study. Subjects with no history of ulcers or neurological disorders (except neuropathy) [12], and are able to walk freely without walking aids [61] are included in this experiment. The exclusion criteria are those with active ulcers at the time of the experiment and severe foot deformities, such as cavus foot and Charcot arthropathy, have cardiovascular and vascular diseases, claudication, retinopathy, nephropathy, lower limb amputation, and other orthopaedic problems (e.g., fractures) or neurological (e.g., stroke) impairment that could affect gait [12]. This study was approved by the Human Subjects Ethics Sub-committee of The Hong Kong Polytechnic University (Reference Number: HSEARS20200128001). Experimental requirements and written informed consent are provided to all of the participants before participation in the study. The descriptive statistics of the 52 participants including age, body mass index (BMI), foot size and years of diagnosis are listed in Table 1.

2) EXPERIMENT

Footprint images of both the left and right feet of each subject were collected by using a Podograph (see Fig. 1). This device

TABLE 1. Descriptive statistics of participants ($n = 52$).

Variable	Mean	SD	Max	Min
Male ($N_1 = 26$)				
Age (years old)	63	6	74	50
BMI (kg/m2)	23.7	2.4	28.2	19.3
Foot size (EUR)	41	1	44	38
Years of diagnosis (DM)	10	8	28	1
Female ($N_2 = 26$)				
Age (years)	65	5	75	56
BMI (kg/m2)	23.2	3.7	33.4	18.2
Foot size (EUR)	39	1	42	37
Years of diagnosis (DM)	13	14	63	1

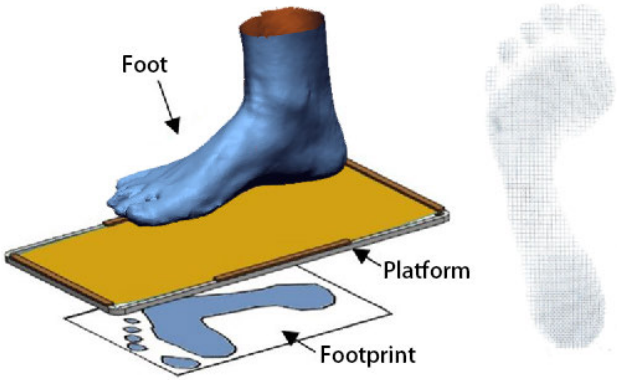

FIGURE 1. Ink footprint image from podograph.

is used to take the outline of the foot and imprint of the sole. The subjects were instructed to step onto the platform of the Podograph in their bare feet for 10 s without any movement, so that the body weight is evenly distributed onto both feet as much as possible during this procedure. To ensure that the footprints have a consistent quality, the same ink and device was used to make sure the constant viscosity held across all footprint samples. Additionally, the footprint images were collected by the same operator who is well trained to use the device, to ensure a consistent manner to control the pressure used, reducing variability from this factor.

Studies [62], [63] have concluded that polyurethane (PUR), ethylene vinyl acetate (EVA) and polyethylene (PE) are most frequently used by orthopaedic technicians in current clinical practice. They are all foam materials with a different structure and properties. PUR foam is soft due to an open cell structure, which allows breathability and offers superior shock absorption in comparison to the other foams. EVA and PE have a closed cell structure so that they are more rigid than PUR, but also have better shock absorbing quality. Four commonly used insole materials of these three types are involved in this study, see Fig. 2. Aside from footprints, the plantar pressure of both the left and right feet of each subject in their bare feet and wearing the 3D insoles designed with 4 different kinds of materials (see Fig. 2) at their self-selected

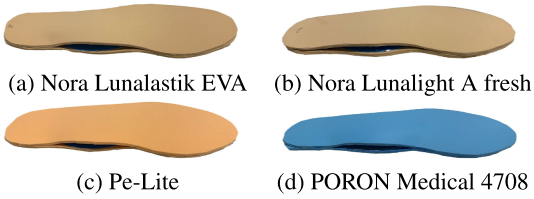

FIGURE 2. 3D insoles designed with different materials used for insoles.

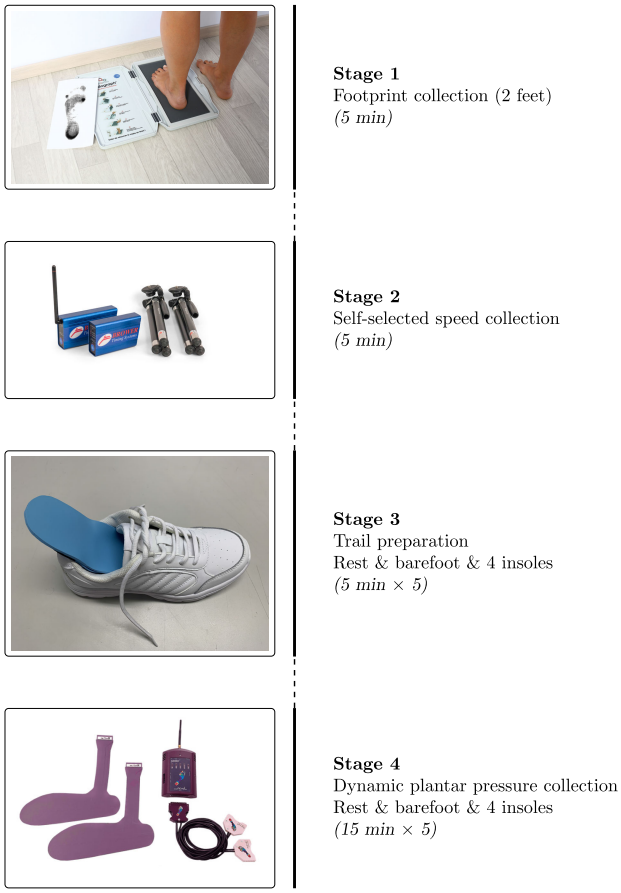

FIGURE 3. Experimental flow.

walking speed was also collected respectively by using the in-shoe Pedar® system. The Pedar insole has been calibrated by technicians before the wear trial experiment. The sensor insoles of the in-shoe Pedar® system could be secured and embedded in the footwear to record the plantar pressure between the foot and the insole during standing and walking. After applying the sensor, the subjects were required to repeat walking back and forth until it is natural. To minimize the order effect, the 5 experiment conditions for plantar pressure collection are randomized and recorded 3 times for each condition. The experiment environment was controlled at about 25 °C air temperature and 55% humidity condition during the experiment. The flow of the entire experiment is illustrated in Fig. 3.

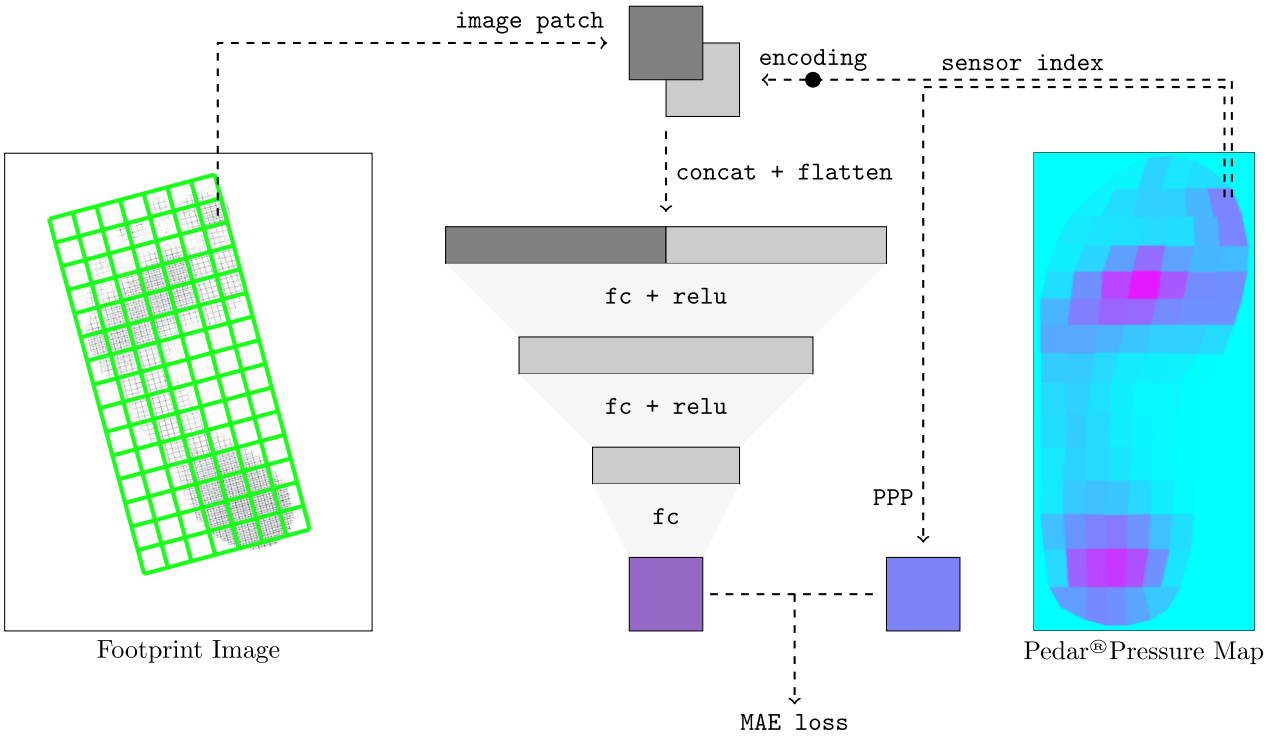

FIGURE 4. Flowchart of model training. Noted that concatenation, fully connected layer, ReLU activation, and mean peak plantar pressure are abbreviated as `concat`, `fc`, `relu`, and `PPP`, respectively.

3) DATA PROCESSING

The dynamic plantar pressure of each condition was collected by using an in-shoe Pedar® system, which consists of 99 sensors on each insole. The raw plantar pressure data collected by each sensor is a time series of pressure values, representing its dynamic changes during walking. As a representative metric of the pressure level in the sensing area, the mean peak plantar pressure (PPP) of each sensor in the left and right feet in 3 complete stance phases for each trial was calculated, resulting to a pressure map. The pressure values were normalized with the maximum sensing range of the device (600 kPa), yielding normalized pressure values in [0, 1] [64].

The footprint images were scanned with a printer to convert them to grayscale images before inputting to the model. In total, 520 footprint image-plantar pressure distribution pairs were collected from 52 subjects, each with left & right feet footprint-pressure pairs under 5 conditions (bare foot + 4 insoles in Fig. 2). The *diabetes-footprint-to-pressure* dataset can be accessed via `[data repo link]`.

B. PATCH-BASED MLP WITH LOCALIZATION EMBEDDING

The overall structure of the proposed model is depicted in Fig. 4. Following is the detailed description of each components.

1) CONSTRUCTING INK DENSITY PATCH-PLANTAR PRESSURE PAIRS

One of severe challenges to train the model to learn the correspondence between footprint ink density and plantar pressure is the lack of data samples. As described in subsection III-A, the 520 pairs of footprint-pressure pairs are separated to 5 conditions (bare foot + 4 insoles in Fig. 2), i.e. only 104 samples for each condition. To address this issue, the following data augmentation scheme is implemented:

(a) The foot contact area in the footprint image is located and segmented using canny edge detection algorithm [65], warped to a rectangle, and resampled by a 500 × 300 image grids.
(b) Since the sensor insole of the in-shoe Pedar® system is arranged by 99 sensors, in order to better match the ink information of footprint with each sensor, the footprint was divided into 15 × 7 (row × column) patches.
(c) The plantar pressure collected by the 99 sensors are distributed to the 15 × 7 patches. Here, we only roughly assign a nearby sensor to a footprint image patch with the index number of the sensor being recorded. Experimental results show that such a simple assignment scheme suffice to deliver satisfying results, although a more sophisticated sensor assignment and pressure distribution scheme may be beneficial. The footprint image patches, distributed pressure value and the index

number of the sensor together constitute the ink density patch-plantar pressure pair.

This approach has 2 advantages: (1) it increases the number of samples by around 100 times, reaching 10,400 data samples for each condition; and (2) it transforms the difficult whole image pressure regression problem into a simpler patch-based local pressure regression problem.

2) LOCALIZATION EMBEDDING

The drawback of transforming the whole image regression to patch based local regression is that the localization information of each locale is lost, which could mislead the model to learn a blurry relationship between ink density and plantar pressure. To address this issue, the index number of the sensor that the pressure value is distributed from is embedded to a 2D tensor with the same size of the image patch, and then concatenated with the image patch. This component is in sprit similar to the Word2Vec model proposed by Mikolov et al. [66] and the positional encodings in the Transformer by Vaswani et al. [67] and NeRF by Mildenhall et al. [68].

3) MULTILAYER PERCEPTRON

The footprint image patch concatenated with the localization embedding is flatten as a 1-d vector as the input to a stack of fully connected layers with ReLU activation [41], as shown in Fig. 4. The number of neurons following the input layer are set as 512, 512, 256, 256, 128, 128, respectively. Mean absolute error (MAE) loss is used as the loss function to train the model.

C. IMPLEMENTATION DETAILS

The training data is randomly distributed for the training, development and testing sets with the ratio of 6:2:2. Training and testing is executed on a Window 11 Pro computer system with a 64-bit operating system and x64-based processor, Intel (R) Core (TM) i7-11700K CPU @ 3.6 GHz, 16 GB RAM, with a Nvidia GeForce RTX 3060 GPU with 12 GB memory. The Adam optimizer [69] is used with a learning rate of 0.008. Training epochs is set to 400, while the batch size is 64. Python 3.8.12 with PyTorch 1.10.0 [70] has been used in learning environments for training and model testing. 5 models for each condition (bare foot + 4 insoles in Fig. 2) were developed for each experimental scenario using the same hyper-parameters. Code has been released at `[code repo link]`.

IV. RESULT

A. COMPARISON BASELINES

As discussed in section I, to the best of our knowledge, there is no direct prior work on quantitatively predicting the plantar pressure from the ink footprints. To validate the proposed model, we construct a series of comparison baselines with some widely used convolutional network structures, including AlexNet [41], DarkNet [42], and ResNet [71], all with versions with and without localization embedding (subsubsection III-B2). For our patch based MLP, to validate the network configurations, the full 7 layers version and the 5, 3 layers versions are constructed by removing later layers accordingly. To validate the effectiveness of localization embedding, each of these versions consists two sub-versions with and without localization embedding. The models are trained and evaluated on the same dataset as the proposed model. The MAE and AUC are presented in Table 2, showing that our proposed model outperforms all these comparison baselines.

TABLE 2. Evaluation results of patch level predictions.

Model	MAE (%) ↓	AUC (%) ↑
AlexNet	7.23	92.34
AlexNet-emb	4.75	94.79
DarkNet	7.81	91.75
DarkNet-emb	6.66	92.90
ResNet	7.00	92.56
ResNet-emb	5.79	93.76
MLP-3	7.07	92.50
MLP-3-emb	4.54	94.98
MLP-5-emb	4.46	95.07
MLP-7-emb	**4.45**	**95.08**

Models with localization embedding are denoted with *-emb*. Number of layers of our proposed patch based MLP is denoted as the digit after the model name -<*layer*>. The mean absolute error (MAE) is reported as percentage with respect to the Pedar® sensor range (600 kPa). The area under the ROC curve (AUC) is also presented as percentage up to 100%. The best performance of each metric is highlighted in bold.

B. PATCH LEVEL EVALUATION

1) MAE

Since the network is trained on patches of footprint-pressure pairs, the MAE is calculated on the patch level. As shown in Table 2, all model structures present improved accuracies by leveraging the localization embedding, validating its effectiveness. Among all models, only AlexNet with localization embedding achieves accuracy comparable to our model, but it is still slightly inferior. Among all variants of the proposed batch based MLP models, the 7 layer version with localization embedding achieves the highest accuracy with an MAE of 4.45% of the sensor range, which can be considered sufficient for the clinical use in assessing the plantar pressure pattern.

2) ROC & AUC

Except for the averaged absolute error metric, we also examined the receiver operating characteristic (ROC) curve of the models by considering the patches with MAE under certain threshold as positive predictions to illustrate the models' performance against different accuracy thresholds. Following this setting, the area under the ROC curve (AUC) values are also computed as shown in Table 2. As shown in Fig. 5, all models with localization embedding present better performance than those without localization embedding and our proposed methods set the upper bound of all other methods. The AUC of the proposed model

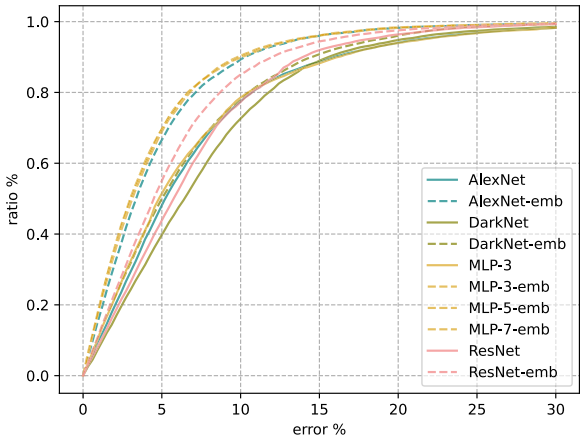

FIGURE 5. ROC curves of patch level predictions. Curves of different model structures are shown in different colors. Models with localization embedding are shown in dashed lines, while those without localization embedding are shown in solid lines.

TABLE 3. MAE of different conditions.

	MAE (%) ↓				
Model	BF	Lunalastik	Lunalight	PElite	Poron
AlexNet	9.48	6.32	7.65	6.88	5.83
AlexNet-emb	5.72	4.32	5.24	4.60	3.87
DarkNet	10.29	6.84	8.17	7.13	6.64
DarkNet-emb	6.12	6.04	8.75	8.36	4.02
ResNet	–	6.81	7.86	7.13	6.18
ResNet-emb	7.13	5.37	5.40	5.88	5.19
MLP-3	9.34	6.21	7.43	6.80	5.55
MLP-3-emb	5.68	4.02	4.92	4.32	3.78
MLP-5-emb	5.56	**3.99**	4.89	4.29	**3.57**
MLP-7-emb	**5.51**	4.03	**4.85**	**4.25**	3.60

For concision, the conditions are abbreviated as BF, Lunalastik, Lunalight, PElite, and Poron for barefoot, Nora Lunalastik EVA, Nora Lunalight A fresh, Pe-Lite, and PORON Medical 4708, respectively. The mean absolute error (MAE) is reported as percentage with respect to the Pedar® sensor range (600 kPa). The best performance of each metric is highlighted in bold.

is significantly higher than the comparison baselines, with the 7 layer embedded version achieves the highest AUC of 95.08%, which further validates the effectiveness of the proposed model in predicting plantar pressure from ink footprints.

C. CONDITION LEVEL EVALUATION

Except for patch level evaluation, validating the performance of the proposed method under different insole conditions is crucial for clinical applications. The MAE of the proposed model under different conditions are presented in Table 3. Results show that the proposed model outperforms all comparison baselines under all conditions, with the 5 and 7 layer versions achieves the best accuracy with an MAEs from 3.57%–5.51% of the sensor range. The proposed model also shows a consistent performance across different conditions, illustrating its robustness and generalization ability.

D. INSTANCE LEVEL EVALUATION

Previous results have shown the effectiveness of the proposed model in predicting the plantar pressure from the ink footprints in a patch level setting. The next question is does aggregating all patch level predictions produce a reliable and accurate result for the whole footprint instance. Fig. 6 shows some prediction samples of different models as well as the ground-truth plantar pressure maps. As shown in Fig. 6b, models without localization embedding tends to generate blurry and flat pressure distribution, whereas models with localization embedding, as shown in Fig. 6a, present more accurate and detailed predictions. Among the models with localization embedding, DarkNet and ResNet tends to generate noised and discontinued pressure distribution, while the proposed patch based MLP model and the AlexNet present more smooth and similar pressure distribution to the ground-truth. This result indicates that both our proposed method and AlexNet are capable of qualitatively recovering the plantar pressure distribution from the ink footprints, while according to previous results our proposed model provides more quantitatively accurate results.

V. DISCUSSION

Footprints have been widely studied as a source of information of activities and personal characteristics. They are generated on the contact interface between the foot and the ground by the loads from body weight and body movement, which has substantial potential valuable information for studying the shape and function of the foot itself, but also of value in analysing gait and general body movements [72]. This study has formulated artificial intelligent (AI) models for dynamic plantar pressure prediction through the use of ink images of the feet to quantify the relationship between the two based on patch based MLP model. The results indicate that the predicted overall and regional plantar pressure distributions are in good agreement with the experimental values. The generated plantar pressure distribution can be used to estimate different offloading effects with 4 different insole materials, leading to a better understanding of the insole-foot interaction as well as provide information for clinicians to prescribe the most suitable insole for diabetic patients.

To the best of our knowledge, this study is the first study to use the ink footprint image to predict the quantitative plantar pressure value induced by insole intervention for diabetic patients. Compared to traditional laboratory wear trials and time-consuming FE prediction models relying on complicated parameterization, the new approach can help clinicians provide accurate insole recommendations - which can even be specific to each plantar region. Nevertheless, there are some limitations to our current approach. Firstly, the dataset is relatively small. Secondly, the ink footprint images are not perfectly aligned with the Pedar sensor insole area. More sophisticated pressure sensor-footprint

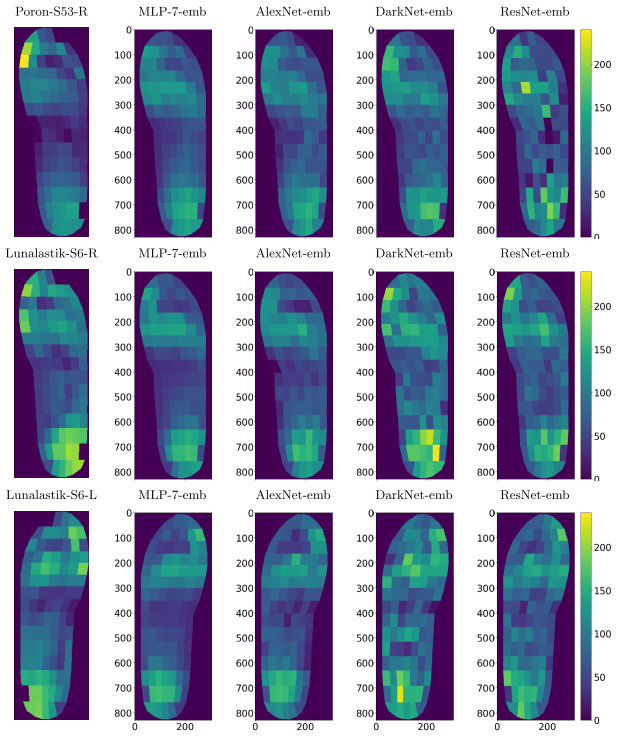

(a) w/ embedding

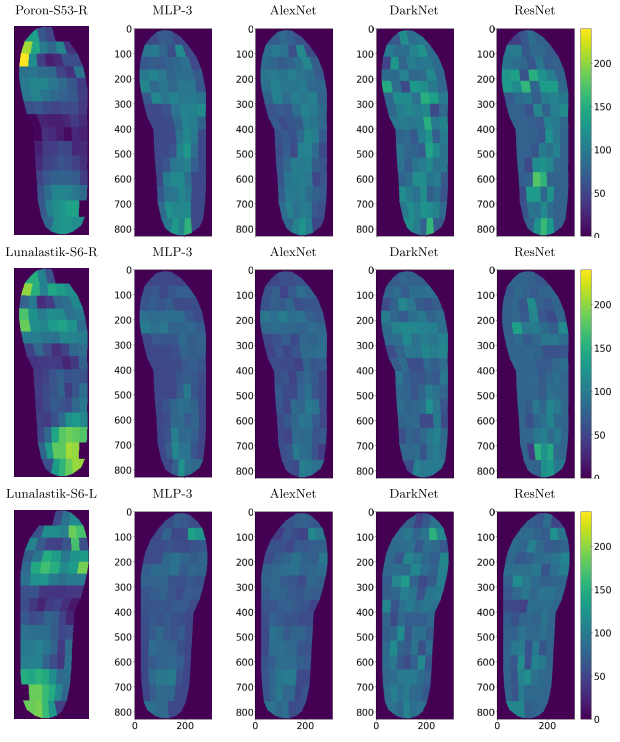

(b) w/o embedding

FIGURE 6. Prediction samples. The first column shows the ground-truth pressure maps tagged with *<condition>-<subject>-<foot>*. The following columns show the predicted pressure maps from: (a) models with localization embedding; and (b) models without localization embedding.

patch association scheme may further improve the prediction accuracy. Thirdly, the current study only considers the effect of insole materials on plantar pressure. Future work may consider other factors such as insole thickness, hardness, and shape.

VI. CONCLUSION

We proposed an innovative approach to predict the plantar pressure distribution from footprint images in various insole conditions based on patch based MLP with localization embedding. Though evaluation shows that the proposed method outperforms all comparison baselines in terms of patch level pressure prediction accuracy as well as the overall plantar pressure pattern.

The proposed model can be leveraged to efficiently recover the contact plantar pressure distribution between the insole and the foot plantar with low-cost footprints. It provides a tool to better understand the complex interactions between the plantar of the foot of individuals and the 3D orthotic insole made of various insole materials with different density, softness, and other properties. The plantar pressure profile when wearing a particular insole material can be prominently visualized and quantitatively predicted, as well as the contact plantar pressure distribution over different regions of the foot, leading to more efficient and patient-specific insole recommendations for diabetic patients in fulfillment of their clinical needs.

REFERENCES

[1] Y. Duan, W. Ren, L. Xu, W. Ye, Y.-K. Jan, and F. Pu, "The effects of different accumulated pressure-time integral stimuli on plantar blood flow in people with diabetes mellitus," *BMC Musculoskeletal Disorders*, vol. 22, no. 1, p. 554, Jun. 2021, doi: 10.1186/s12891-021-04437-9.

[2] B. J. Beuker, R. W. Van Deursen, P. Price, E. A. Manning, J. G. Van Baal, and K. G. Harding, "Plantar pressure in off-loading devices used in diabetic ulcer treatment," *Wound Repair Regener.*, vol. 13, no. 6, pp. 537–542, Nov. 2005, doi: 10.1111/j.1524-475x.2005.00075.x.

[3] S. A. Bus, "Priorities in offloading the diabetic foot," *Diabetes/Metabolism Res. Rev.*, vol. 28, no. S1, pp. 54–59, Jan. 2012, doi: 10.1002/dmrr.2240.

[4] S. Ahmed, A. Barwick, P. Butterworth, and S. Nancarrow, "Footwear and insole design features that reduce neuropathic plantar forefoot ulcer risk in people with diabetes: A systematic literature review," *J. Foot Ankle Res.*, vol. 13, no. 1, p. 30, Jan. 2020, doi: 10.1186/s13047-020-00400-4.

[5] R. Collings, J. Freeman, J. M. Latour, S. Glasser, and J. Paton, "Footwear and insole design features to prevent foot ulceration in people with diabetes: A systematic review protocol," *JBI Database Systematic Rev. Implement. Rep.*, vol. 15, no. 7, pp. 1824–1834, Jul. 2017, doi: 10.11124/jbisrir-2016-003291.

[6] J. J. van Netten, P. A. Lazzarini, D. G. Armstrong, S. A. Bus, R. Fitridge, K. Harding, E. Kinnear, M. Malone, H. B. Menz, B. M. Perrin, K. Postema, J. Prentice, K. Schott, and P. R. Wraight, "Diabetic foot Australia guideline on footwear for people with diabetes," *J. Foot Ankle Res.*, vol. 11, no. 1, p. 2, Jan. 2018, doi: 10.1186/s13047-017-0244-z.

[7] J. T.-M. Cheung and M. Zhang, "Parametric design of pressure-relieving foot orthosis using statistics-based finite element method," *Med. Eng. Phys.*, vol. 30, no. 3, pp. 269–277, Apr. 2008, doi: 10.1016/j.medengphy.2007.05.002.

[8] S. A. Bus, R. Haspels, and T. E. Busch-Westbroek, "Evaluation and optimization of therapeutic footwear for neuropathic diabetic foot patients using in-shoe plantar pressure analysis," *Diabetes Care*, vol. 34, no. 7, pp. 1595–1600, Jun. 2011, doi: 10.2337/dc10-2206.

[9] C. Gerlach, D. Krumm, M. Illing, J. Lange, O. Kanoun, S. Odenwald, and A. Hübler, "Printed MWCNT-PDMS-Composite pressure sensor system for plantar pressure monitoring in ulcer prevention," *IEEE Sensors J.*, vol. 15, no. 7, pp. 3647–3656, Jul. 2015, doi: 10.1109/JSEN.2015.2392084.

[10] X. Li, H. Huang, J. Wang, Y. Yu, and Y. Ao, "The analysis of plantar pressure data based on multimodel method in patients with anterior cruciate ligament deficiency during walking," *BioMed Res. Int.*, vol. 2016, pp. 1–12, Jan. 2016, doi: 10.1155/2016/7891407.

[11] M. J. Hessert, M. Vyas, J. Leach, K. Hu, L. A. Lipsitz, and V. Novak, "Foot pressure distribution during walking in young and old adults," *BMC Geriatrics*, vol. 5, no. 1, p. 8, May 2005, doi: 10.1186/1471-2318-5-8.

[12] I. C. N. Sacco, A. N. Hamamoto, L. M. G. Tonicelli, R. Watari, N. R. S. Ortega, and C. D. Sartor, "Abnormalities of plantar pressure distribution in early, intermediate, and late stages of diabetic neuropathy," *Gait Posture*, vol. 40, no. 4, pp. 570–574, Sep. 2014, doi: 10.1016/j.gaitpost.2014.06.018.

[13] G. Gijon-Nogueron, A. Marchena-Rodriguez, J. Montes-Alguacil, and A. M. Evans, "Evaluation of the paediatric foot using footprints and foot posture index: A cross-sectional study," *J. Paediatrics Child Health*, vol. 56, no. 2, pp. 201–206, Jul. 2019, doi: 10.1111/jpc.14558.

[14] L. Gutiérrez-Vilahú and M. Guerra-Balic, "Footprint measurement methods for the assessment and classification of foot types in subjects with down syndrome: A systematic review," *J. Orthopaedic Surg. Res.*, vol. 16, no. 1, p. 537, Aug. 2021, doi: 10.1186/s13018-021-02667-0.

[15] S. Xiong, R. S. Goonetilleke, C. P. Witana, T. W. Weerasinghe, and E. Y. L. Au, "Foot arch characterization: A review, a new metric, and a comparison," *J. Amer. Podiatric Med. Assoc.*, vol. 100, 1, pp. 14–24, 2010. [Online]. Available: https://api.semanticscholar.org/CorpusID:5734992

[16] S. R. Urry and S. C. Wearing, "A comparison of footprint indexes calculated from ink and electronic footprints," *J. Amer. Podiatric Med. Assoc.*, vol. 91, no. 4, pp. 203–209, Apr. 2001, doi: 10.7547/87507315-91-4-203.

[17] S. Lt, C. De, and M. Corbett, "The longitudinal arch. A survey of eight hundred and eighty-two feet in normal children and adults," *J. Bone Joint Surg. Amer.*, vol. 69, no. 3, pp. 426–428, 1987. [Online]. Available: https://api.semanticscholar.org/CorpusID:35584507

[18] K.-H. Su, T. Kaewwichit, C.-H. Tseng, and C.-C. Chang, "Automatic footprint detection approach for the calculation of arch index and plantar pressure in a flat rubber pad," *Multimedia Tools Appl.*, vol. 75, no. 16, pp. 9757–9774, Aug. 2015, doi: 10.1007/s11042-015-2796-x.

[19] Y. Lecun, L. Bottou, Y. Bengio, and P. Haffner, "Gradient-based learning applied to document recognition," *Proc. IEEE*, vol. 86, no. 11, pp. 2278–2324, Jan. 1998, doi: 10.1109/5.726791.

[20] C. Szegedy, W. Liu, Y. Jia, P. Sermanet, S. Reed, D. Anguelov, D. Erhan, V. Vanhoucke, and A. Rabinovich, "Going deeper with convolutions," in *Proc. IEEE Conf. Comput. Vis. Pattern Recognit. (CVPR)*, Jun. 2015, pp. 1–9, doi: 10.1109/CVPR.2015.7298594.

[21] K. Simonyan and A. Zisserman, "Very deep convolutional networks for large-scale image recognition," in *Computational and Biological Learning Society*, 2015, pp. 1–14.

[22] Y. M. Mohialden, N. M. Hussien, S. A. Salman, A. Bahaaulddin A. Alwahhab, and M. Ali, "Enhancing agriculture crop classification with deep learning," *Babylonian J. Artif. Intell.*, vol. 2024, pp. 20–26, Mar. 2024, doi: 10.58496/bjai/2024/004.

[23] R. Girshick, J. Donahue, T. Darrell, and J. Malik, "Rich feature hierarchies for accurate object detection and semantic segmentation," in *Proc. IEEE Conf. Comput. Vis. Pattern Recognit.*, Jun. 2014, pp. 580–587, doi: 10.1109/CVPR.2014.81.

[24] R. Girshick, "Fast R-CNN," in *Proc. IEEE Int. Conf. Comput. Vis. (ICCV)*, Dec. 2015, pp. 1440–1448, doi: 10.1109/ICCV.2015.169.

[25] S. Ren, K. He, R. Girshick, and J. Sun, "Faster R-CNN: Towards real-time object detection with region proposal networks," *IEEE Trans. Pattern Anal. Mach. Intell.*, vol. 39, no. 6, pp. 1137–1149, Jun. 2017, doi: 10.1109/TPAMI.2016.2577031.

[26] T.-Y. Lin, P. Dollár, R. Girshick, K. He, B. Hariharan, and S. Belongie, "Feature pyramid networks for object detection," in *Proc. IEEE Conf. Comput. Vis. Pattern Recognit. (CVPR)*, Jul. 2017, pp. 936–944, doi: 10.1109/CVPR.2017.106.

[27] O. Ronneberger, P. Fischer, and T. Brox, *U-Net: Convolutional Networks for Biomedical Image Segmentation*. Cham, Switzerland: Springer, 2015, pp. 234–241, doi: 10.48550/arXiv.1505.04597.

[28] X. Zhu, Z. Lei, X. Liu, H. Shi, and S. Z. Li, "Face alignment across large poses: A 3D solution," in *Proc. IEEE Conf. Comput. Vis. Pattern Recognit. (CVPR)*, Jun. 2016, pp. 146–155, doi: 10.1109/CVPR.2016.23.

[29] R. A. Güler, G. Trigeorgis, E. Antonakos, P. Snape, S. Zafeiriou, and I. Kokkinos, "DenseReg: Fully convolutional dense shape regression in-the-wild," in *Proc. IEEE Conf. Comput. Vis. Pattern Recognit. (CVPR)*, Jul. 2017, pp. 2614–2623, doi: 10.1109/CVPR.2017.280.

[30] R. A. Güler, N. Neverova, and I. Kokkinos, "DensePose: Dense human pose estimation in the wild," in *Proc. IEEE/CVF Conf. Comput. Vis. Pattern Recognit.*, Jun. 2018, pp. 7297–7306, doi: 10.1109/CVPR.2018.00762.

[31] S. K. Kalagotla, S. V. Gangashetty, and K. Giridhar, "A novel stacking technique for prediction of diabetes," *Comput. Biol. Med.*, vol. 135, Aug. 2021, Art. no. 104554, doi: 10.1016/j.compbiomed.2021.104554.

[32] R. Qamar and B. Ali Zardari, "Artificial neural networks: An overview," *Mesopotamian J. Comput. Sci.*, vol. 2023, pp. 130–139, Aug. 2023, doi: 10.58496/mjcsc/2023/015.

[33] S. M. Alqaraghuli and O. Karan, "Using deep learning technology based energy-saving for software defined wireless sensor networks (SDWSN) framework," *Babylonian J. Artif. Intell.*, vol. 2024, pp. 34–45, Apr. 2024. [Online]. Available: https://mesopotamian.press/journals/index.php/BJAI/article/view/378

[34] M. Abdar, N. Y. Yen, and J. C.-S. Hung, "Improving the diagnosis of liver disease using multilayer perceptron neural network and boosted decision trees," *J. Med. Biol. Eng.*, vol. 38, no. 6, pp. 953–965, Dec. 2017, doi: 10.1007/s40846-017-0360-z.

[35] S. Ahmadian, S. M. J. Jalali, S. Raziani, and A. Chalechale, "An efficient cardiovascular disease detection model based on multilayer perceptron and moth-flame optimization," *Expert Syst.*, vol. 39, no. 4, Dec. 2021, Art. no. e12914, doi: 10.1111/exsy.12914.

[36] D. Ciresan, A. Giusti, L. Gambardella, and J. Schmidhuber, "Deep neural networks segment neuronal membranes in electron microscopy images," in *Proc. Adv. Neural Inf. Process. Syst.*, vol. 25, F. Pereira, C. Burges, L. Bottou, and K. Weinberger, Eds., Red Hook, NY, USA: Curran Associates, Inc., 2012, pp. 2843–2851. [Online]. Available: https://proceedings.neurips.cc/paperfiles/paper/2012/file/459a4ddcb586f24efd9395aa7662bc7c-Paper.pdf

[37] M. Adam, E. Y. K. Ng, J. H. Tan, M. L. Heng, J. W. K. Tong, and U. R. Acharya, "Computer aided diagnosis of diabetic foot using infrared thermography: A review," *Comput. Biol. Med.*, vol. 91, pp. 326–336, Dec. 2017, doi: 10.1016/j.compbiomed.2017.10.030.

[38] M. Fatima and M. Pasha, "Survey of machine learning algorithms for disease diagnostic," *J. Intell. Learn. Syst. Appl.*, vol. 9, no. 1, pp. 1–16, 2017, doi: 10.4236/jilsa.2017.91001.

[39] G. Battineni, G. G. Sagaro, N. Chinatalapudi, and F. Amenta, "Applications of machine learning predictive models in the chronic disease diagnosis," *J. Personalized Med.*, vol. 10, no. 2, p. 21, Mar. 2020, doi: 10.3390/jpm10020021.

[40] R. Jain, A. Chotani, and G. Anuradha, *Data Analytics in Biomedical Engineering and Healthcare*. Amsterdam, The Netherlands: Elsevier, 2021, pp. 145–161, doi: 10.1016/B978-0-12-819314-3.00010-0.

[41] A. Krizhevsky, I. Sutskever, and G. E. Hinton, "Imagenet classification with deep convolutional neural networks," in *Proc. Adv. Neural Inf. Process. Syst.*, vol. 25, F. Pereira, C. Burges, L. Bottou, and K. Weinberger, Eds., Red Hook, NY, USA: Curran Associates, 2012, pp. 84–90. [Online]. Available: https://proceedings.neurips.cc/paperfiles/paper/2012/file/c399862d3b9d6b76c8436e924a68c45b-Paper.pdf

[42] J. Redmon, S. Divvala, R. Girshick, and A. Farhadi, "You only look once: Unified, real-time object detection," in *Proc. IEEE Conf. Comput. Vis. Pattern Recognit. (CVPR)*, Jun. 2016, pp. 779–788, doi: 10.1109/CVPR.2016.91.

[43] F. Mun and A. Choi, "Deep learning approach to estimate foot pressure distribution in walking with application for a cost-effective insole system," *J. NeuroEng. Rehabil.*, vol. 19, no. 1, p. 4, Jan. 2022, doi: 10.1186/s12984-022-00987-8.

[44] M. Nouman, T. Dissaneewate, D. Y. R. Chong, and S. Chatpun, "Effects of custom-made insole materials on frictional stress and contact pressure in diabetic foot with neuropathy: Results from a finite element analysis," *Appl. Sci.*, vol. 11, no. 8, p. 3412, Apr. 2021, doi: 10.3390/app11083412.

[45] M. J. Ghazali, X. Ren, A. Rajabi, W. F. H. W. Zamri, N. M. Mustafah, and J. Ni, "Finite element analysis of cushioned diabetic footwear using ethylene vinyl acetate polymer," *Polymers*, vol. 13, no. 14, p. 2261, Jul. 2021, doi: 10.3390/polym13142261.

[46] S. Paul, D. P. Kumar, and B. Siva, "Material analysis for therapeutic insoles—A short report," *Leprosy Rev.*, vol. 92, no. 1, pp. 75–81, Mar. 2021, doi: 10.47276/lr.92.1.75.

[47] Z. Taha, M. S. Norman, S. F. S. Omar, and E. Suwarganda, "A finite element analysis of a human foot model to simulate neutral standing on ground," *Proc. Eng.*, vol. 147, pp. 240–245, Jan. 2016, doi: 10.1016/j.proeng.2016.06.240.

[48] S. T. Strayer, S. R. M. Moghaddam, B. Gusenoff, J. Gusenoff, and K. E. Beschorner, "Contact pressures between the rearfoot and a novel offloading insole: Results from a finite element analysis study," *J. Appl. Biomechanics*, vol. 36, no. 5, pp. 326–333, Oct. 2020, doi: 10.1123/jab.2019-0356.

[49] J. Zhu and J. Forman, "A review of finite element models of ligaments in the foot and considerations for practical application," *J. Biomechanical Eng.*, vol. 144, no. 8, Feb. 2022, Art. no. 080801, doi: 10.1115/1.4053401.

[50] E. Xidias, Z. Koutkalaki, P. Papagiannis, P. Papanikos, and P. Azariadis, *Foot Plantar Pressure Estimation Using Artificial Neural Networks*. Cham, Switzerland: Springer, 2016, pp. 23–32, doi: 10.1007/978-3-319-33111-9_3.

[51] A. Hazari, A. Maiya, I. Agouris, A. Monteiro, and Shivashankara, "Prediction of peak plantar pressure for diabetic foot: The regressional model," *Foot*, vol. 40, pp. 87–91, Sep. 2019, doi: 10.1016/j.foot.2019.06.001.

[52] J. H. Ahroni, E. J. Boyko, and R. C. Forsberg, "Clinical correlates of plantar pressure among diabetic veterans," *Diabetes Care*, vol. 22, no. 6, pp. 965–972, Jun. 1999, doi: 10.2337/diacare.22.6.965.

[53] R. Barn, R. Waaijman, F. Nollet, J. Woodburn, and S. A. Bus, "Predictors of barefoot plantar pressure during walking in patients with diabetes, peripheral neuropathy and a history of ulceration," *PLoS ONE*, vol. 10, no. 2, Feb. 2015, Art. no. e0117443, doi: 10.1371/journal.pone.0117443.

[54] O. A. Fawzy, A. I. Arafa, M. A. E. Wakeel, and S. H. A. Kareem, "Plantar pressure as a risk assessment tool for diabetic foot ulceration in Egyptian patients with diabetes," *Clin. Med. Insights, Endocrinol. Diabetes*, vol. 7, Jan. 2014, Art. no. CMED.S17088, doi: 10.4137/cmed.s17088.

[55] W. S. McCulloch and W. Pitts, "A logical calculus of the ideas immanent in nervous activity," *Bull. Math. Biophys.*, vol. 5, no. 4, pp. 115–133, Dec. 1943, doi: 10.1007/bf02478259.

[56] D. Devarapalli, A. Apparao, M. Narasinga Rao, A. Kumar, and G. Sridhar, "A multi-layer perceptron (MLP) neural network based diagnosis of diabetes using brain derived neurotrophic factor (BDNF) levels," *Int. J. Adv. Comput*, vol. 35, no. 12, pp. 1–6, 2012.

[57] D. E. Rumelhart, G. E. Hinton, and R. J. Williams, "Learning representations by back-propagating errors," *Nature*, vol. 323, no. 6088, pp. 533–536, Oct. 1986, doi: 10.1038/323533a0.

[58] S. K. Mohapatra, J. K. Swain, and M. N. Mohanty, *Detection Diabetes Using Multilayer Perceptron*. Singapore: Springer, Sep. 2018, pp. 109–116, doi: 10.1007/978-981-13-2182-5_11.

[59] H. Bani-Salameh, S. M. Alkhatib, M. Abdalla, M. Al-Hami, R. Banat, H. Zyod, and A. J. Alkhatib, "Prediction of diabetes and hypertension using multi-layer perceptron neural networks," *Int. J. Model., Simul., Sci. Comput.*, vol. 12, no. 2, Jan. 2021, Art. no. 2150012, doi: 10.1142/s1793962321500124.

[60] U. M. Butt, S. Letchmunan, M. Ali, F. H. Hassan, A. Baqir, and H. H. R. Sherazi, "Machine learning based diabetes classification and prediction for healthcare applications," *J. Healthcare Eng.*, vol. 2021, pp. 1–17, Sep. 2021, doi: 10.1155/2021/9930985.

[61] S. A. Bus, R. W. M. van Deursen, R. V. Kanade, M. Wissink, E. A. Manning, J. G. van Baal, and K. G. Harding, "Plantar pressure relief in the diabetic foot using forefoot offloading shoes," *Gait Posture*, vol. 29, no. 4, pp. 618–622, Jun. 2009, doi: 10.1016/j.gaitpost.2009.01.003.

[62] C. Llobell Andrés, N. Porta Rosas, M. Fernández, A. Camp Faulí, G. Morey Klapsing, and E. Montiel Parreño, "Mechanical characterisation of insole materials used for diabetic insole orthotics," in *Proc. 4th IASTED Int. Conf. Biomechanics, BioMech*, vol. 2006, 2006, pp. 38–43.

[63] J. M. Gerrard, D. R. Bonanno, G. A. Whittaker, and K. B. Landorf, "Effect of different orthotic materials on plantar pressures: A systematic review," *J. Foot Ankle Res.*, vol. 13, no. 1, p. 35, Jan. 2020, doi: 10.1186/s13047-020-00401-3.

[64] H.-C. Chen, Sunardi, Y.-K. Jan, B.-Y. Liau, C.-Y. Lin, J. Y. Tsai, C.-T. Li, and C.-W. Lung, "Using deep learning methods to predict walking intensity from plantar pressure images," in *Proc. Int. Conf. Appl. Hum. Factors Ergonom.*, 2021, pp. 270–277. [Online]. Available: https://api.semanticscholar.org/CorpusID:237298579

[65] J. Canny, "A computational approach to edge detection," *IEEE Trans. Pattern Anal. Mach. Intell.*, vol. PAMI-8, no. 6, pp. 679–698, Nov. 1986, doi: 10.1109/TPAMI.1986.4767851.

[66] T. Mikolov, I. Sutskever, K. Chen, G. S. Corrado, and J. Dean, "Distributed representations of words and phrases and their compositionality," in *Proc. Adv. Neural Inf. Process. Syst.*, 2013, pp. 3111–3119.

[67] A. Vaswani, "Attention is all you need," in *Proc. NIPS*, 2017, pp. 6000–6010.

[68] B. Mildenhall, P. P. Srinivasan, M. Tancik, J. T. Barron, R. Ramamoorthi, and R. Ng, "NeRF: Representing scenes as neural radiance fields for view synthesis," in *Proc. ECCV*, 2020, pp. 99–106.

[69] D. P. Kingma and J. Ba, "Adam: A method for stochastic optimization," 2014, *arXiv:1412.6980*.

[70] A. Paszke, S. Gross, F. Massa, A. Lerer, J. Bradbury, G. Chanan, T. Killeen, Z. Lin, N. Gimelshein, L. Antiga, A. Desmaison, A. Köpf, E. Yang, Z. DeVito, M. Raison, A. Tejani, S. Chilamkurthy, B. Steiner, L. Fang, J. Bai, and S. Chintala, *PyTorch: An Imperative Style, High-Performance Deep Learning Library*. Red Hook, NY, USA: Curran Associates, 2019.

[71] K. He, X. Zhang, S. Ren, and J. Sun, "Deep residual learning for image recognition," in *Proc. IEEE Conf. Comput. Vis. Pattern Recognit. (CVPR)*, Jun. 2016, pp. 770–778, doi: 10.1109/CVPR.2016.90.

[72] T. Duckworth, R. P. Betts, C. I. Franks, and J. Burke, "The measurement of pressures under the foot," *Foot Ankle*, vol. 3, no. 3, pp. 130–141, Nov. 1982, doi: 10.1177/107110078200300303.

LI-YING ZHANG received the degree in fashion design and engineering from Taiyuan University of Technology, in 2014, and the M.Sc. degree from Beijing Institute of Fashion Technology, China, in 2019. She is currently pursuing the Ph.D. degree with the School of Fashion and Textiles, The Hong Kong Polytechnic University, Hong Kong. Her research interests include artificial intelligence and ergonomic design.

ZE-QI MA received the B.Sc. degree in computer science from the College of Computer, Guangdong University of Technology, China, in 2022. He is currently pursuing the Ph.D. degree with the School of Fashion and Textiles, The Hong Kong Polytechnic University, Hong Kong, while funded by Laboratory for Artificial Intelligence in Design, Hong Kong. His research interests include multi-view learning, machine learning, and defect detection.

KIT-LUN YICK received the Ph.D. degree from The Hong Kong Polytechnic University (PolyU), Hong Kong, in 1996. She is currently a Full Professor with PolyU. She has carried out several research projects to enhance the design, fit, comfort, and fabrication of patient clothing and footwear. She also committed to research projects on contour fashion and activewear designs based on biomechanical analysis and new material designs and developments for specific support or protective functions and intended end-uses.

PUI-LING LI received the Ph.D. degree from The Hong Kong Polytechnic University (PolyU). She is currently a Postdoctoral Fellow with the School of Fashion and Textiles, PolyU. She is working on a project for the ergonomic design of footwear with an AI-based framework to enhance the plantar pressure and thermal comfort of diabetic patients. Her research interests include anthropometry measurements, material and product evaluation, and insole and footwear development.

JOANNE YIP received the Ph.D. degree from The Hong Kong Polytechnic University (PolyU). She is currently a Full Professor teaching intimate apparel and activewear courses with PolyU. Her research is focused on medical and functional clothing design and their applications. Her research interests include the design of medical textiles and healthcare products by incorporating modern textiles, novel sensors, and garment technologies. More importantly, the medication and surgical procedures to cure the diseases, thus enhancing the quality of life of people and care provided for patients can be improved.

SUN-PUI NG received the Ph.D. degree from the Department of Mechanical Engineering, The Hong Kong Polytechnic University, in 2001. During the master's degree, he was a Research Scholar with the U.S. Army Cold Regions Research and Engineering Laboratory. He specializes in stress and failure analyses of laminated textile composite materials. He has supervised several M.Phil. and Ph.D. students. His latest endeavor is 3D textile design for sound absorption applications.

QI-LONG LIU received the B.Eng. degree in biomedical engineering from the School of Biomedical Engineering, Shenzhen University, China, in 2021. He is currently pursuing the M.Phil. degree with the School of Fashion and Textiles, The Hong Kong Polytechnic University, Hong Kong. His recent research interests include 3D computer vision, human pose estimation, and nonrigid shape correspondence.